

# A HaloTag-Based Reporter System Enabling Two-Color Timestamped Gene Expression Monitoring

Henriette Lämmermann<sup>§\*</sup>

<sup>§</sup>SCS-dsm-firmenich Award for the Best Poster Presentation in Chemical Biology

**Abstract:** Precise gene expression regulation is essential for cellular homeostasis, particularly in stress response pathways. In the endoplasmic reticulum, the unfolded protein response (UPR<sup>ER</sup>) plays an important role in maintaining the protein folding capacity. We developed a chemigenetic gene expression reporter system for BiP/GRP78, a key regulator of the UPR<sup>ER</sup>, based on co-expression of the self-labeling HaloTag protein. We designed a two-color sequential labelling strategy for improved readout sensitivity and applied our system in a high-content screening, identifying a promising novel activator of BiP/GRP78 expression.

**Keywords:** BiP/GRP78 · HaloTag · High-content screening · Reporter gene assay



**Henriette Lämmermann** received her BSc in Chemistry and Biochemistry, as well as her MSc in Biochemistry, from the Ludwig Maximilian University of Munich. During her master's studies, she carried out internships at Bayer Pharmaceuticals and Eurofins Genomics. After completing her master's thesis in the group of Prof. Pablo Rivera Fuentes, she joined the group as a PhD student, working on chemigenetic and

protein-based tools to study gene expression and redox signalling.

Parts of this article have been published in 'Two-Color Timestamping of Gene Expression with a Chemigenetic Reporter System', H. Lämmermann, J. Nguyen, J. F. Tamez-Fernández, F. Kuttler, J. Bortoli Chapalay, M. Chambon, G. Turcatti, P. Rivera-Fuentes, *ChemBioChem* **2025**, *26*, e202500494, <https://doi.org/10.1002/cbic.202500494>.

## 1. Introduction

Cellular homeostasis relies on the precise regulation of gene expression.<sup>[1]</sup> Tightly coordinated gene expression is particularly important in cellular stress response pathways,<sup>[2]</sup> and abnormal regulation is implicated in a range of diseases, including cancer and neurodegenerative diseases.<sup>[3,4]</sup> Therefore, there is significant interest in understanding the detailed mechanisms of these signalling pathways.

### 1.1 ER Stress and BiP/GRP78

In the endoplasmic reticulum (ER), the unfolded protein response (UPR<sup>ER</sup>) plays a critical role in managing the protein folding and processing capacity.<sup>[5]</sup> Upon accumulation of misfolded proteins, transcriptional programs of the UPR<sup>ER</sup> are activated to restore proteostasis.<sup>[6,7]</sup> The binding immunoglobulin protein BiP/GRP78 plays a central role, functioning as a chaperone and a key mediator in UPR<sup>ER</sup> activation.<sup>[7,8]</sup>

### 1.2 Gene Expression Monitoring

Various methods have been developed to monitor gene expression, analysing the transcriptome or protein levels. To study dynamic changes, reporter gene assays have been developed using fusion constructs with luciferase or fluorescent proteins, or by the conditional expression of these reporters under a promoter of interest.<sup>[9]</sup> However, the disruption of protein function due to fusion constructs or the lack of the native chromatin environment present limitations of these systems.

### 1.3 Chemigenetic Reporter System

Here, we summarise our recent report<sup>[10]</sup> of a chemigenetic reporter system that addresses these limitations by integrating the self-labelling HaloTag protein into the genome immediately downstream of the gene encoding BiP/GRP78. Employing an internal ribosome entry site (IRES),<sup>[11,12]</sup> we achieved coexpression of BiP/GRP78 and the reporter HaloTag as separate proteins, preserving the native function of BiP/GRP78 while enabling flexible fluorescent readout. We developed a two-color labelling strategy, providing improved readout sensitivity, and applied the system in a high-content screening, in which a promising novel activator of BiP/GRP78 expression was discovered.

## 2. Results and Discussion

### 2.1 Design of the Reporter System

To establish the reporter system, we inserted the IRES element, followed by HaloTag, downstream of BiP/GRP78 into the genome of HEK293 cells by clustered regularly interspaced short palindromic repeats (CRISPR)/CRISPR-associated 9 (Cas9)-mediated precise integration into target chromosome (CRIS-PITCh) genome editing.<sup>[13]</sup> The IRES element facilitates cap-independent translation initiation,<sup>[14]</sup> allowing translation of HaloTag from the same mRNA as BiP/GRP78. To enable cell selection, the incorporated sequence additionally contained an antibiotic resistance gene (puromycin *N*-acetyltransferase, PuroR),<sup>[15]</sup> separated from HaloTag by the self-cleaving peptide T2A.<sup>[16]</sup>

The insertion of the IRES-HaloTag-T2A-PuroR sequence downstream of BiP/GRP78 thus results in the simultaneous ex-

\*Correspondence: H. Lämmermann, E-mail: henriette.laemmermann@chem.uzh.ch  
Department of Chemistry, University of Zurich, CH-8057 Zurich

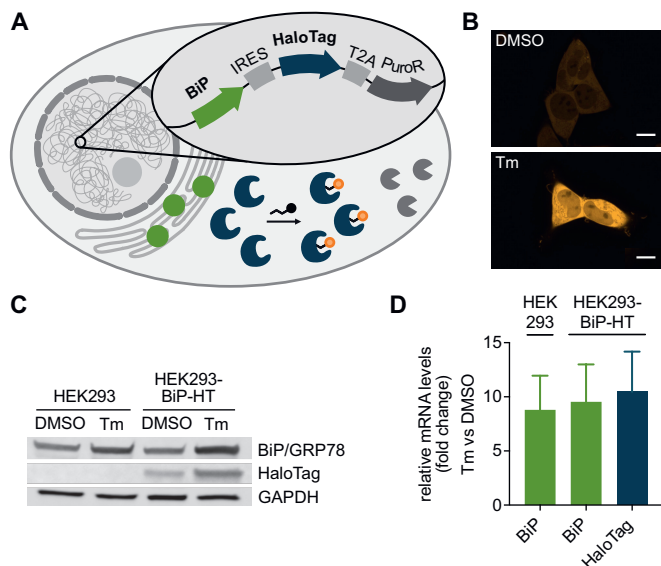


**Fig. 1.** **A** Schematic representation of the chemigenetic reporter system. **B** Live-cell fluorescence images (561 nm) of HEK293-BiP-HT cells incubated with DMSO (0.1%) or tunicamycin (Tm,  $1 \mu\text{g mL}^{-1}$ ) for 16 h. HaloTag was visualized by incubation with the dye MaP555 (100 nM, 30 min). Scale bar:  $10 \mu\text{m}$ . **C** Western blot of protein lysates from HEK293 or HEK293-BiP-HT cells incubated with DMSO (0.1%) or Tm ( $5 \mu\text{g mL}^{-1}$ ) for 24 h. **D** Relative abundances of HaloTag or BiP/GRP78 mRNA comparing Tm-treated ( $2 \mu\text{g mL}^{-1}$ , 6 h) with DMSO-treated (0.1%, 6 h) cells (HEK293 or HEK293-BiP-HT) by RT-qPCR. For each condition, three different samples were prepared, which were each measured in triplicate. Bars represent mean fold change compared to DMSO, error bars represent standard deviation. This figure was adapted from Ref. [10] with permission, Copyright 2025 Wiley-VCH GmbH.

pression of BiP/GRP78, HaloTag, and PuroR as discrete proteins (Fig. 1A).

## 2.2 Validation of the Reporter System

The successful incorporation was first tested *via* fluorescence microscopy. Cells from colonies that had emerged after puromycin selection and single-cell sorting were labelled with the

fluorogenic MaP555 dye,<sup>[17]</sup> which only exhibits fluorescence when HaloTag-bound. Upon treatment with the known ER stress inducer tunicamycin (Tm),<sup>[18,19]</sup> cells showed increased fluorescence intensity compared to cells treated with DMSO (Fig. 1B). We selected the cell line with the strongest response to Tm, named it HEK293-BiP-HT, and further characterised it by Western blot, quantitative reverse transcription polymerase chain reaction (RT-qPCR), and whole-genome sequencing (WGS).

Western blot revealed an increase in the BiP/GRP78 protein amount in Tm-treated HEK293 and HEK293-BiP-HT cells compared to DMSO-treated cells (Fig. 1C). In HEK293-BiP-HT cells, HaloTag and its increase upon Tm treatment were visible.

With RT-qPCR, the relative increase in BiP/GRP78 and HaloTag mRNA was measured by comparing Tm- and DMSO-treated HEK293 and HEK293-BiP-HT cells. Upon Tm-treatment, the amounts of HaloTag and BiP/GRP78 mRNA increased to similar extents, consistent with the fact that BiP/GRP78 and HaloTag are encoded on the same transcript (Fig. 1D). The comparable increase of BiP/GRP78 in both cell lines indicated that transcription of BiP/GRP78 was not affected by genome editing.

WGS confirmed successful heterozygous integration at the target locus with no off-target insertions. This heterozygosity reduces the total amount of HaloTag available for labelling; however, it preserves one almost unmodified allele, minimising potential perturbations to BiP/GRP78 function.

## 2.3 Two-Color Labelling Increases Dynamic Range

Although single-color labelling could distinguish Tm- from DMSO-treated cells, we hypothesised that successive labelling with two colors could detect more subtle expression changes. This is particularly important for BiP/GRP78, which is present at high basal concentrations of  $\sim 0.5 \text{ mM}$  in the ER, making small increases difficult to detect. Additionally, temporal separation of signals would be beneficial for studying genes with large cell-to-cell expression variability.

We designed the following protocol (Fig. 2A): First, cells are incubated with MaP555 to label the existing HaloTag, representing the basal level of BiP/GRP78. After washing to remove unbound dye, cells are treated with a stimulus (*e.g.* Tm) in the presence of a second dye, a silicon rhodamine bromoalkane (SiR-Br) for fast HaloTag labelling (Fig. 2B). These two fluorogenic

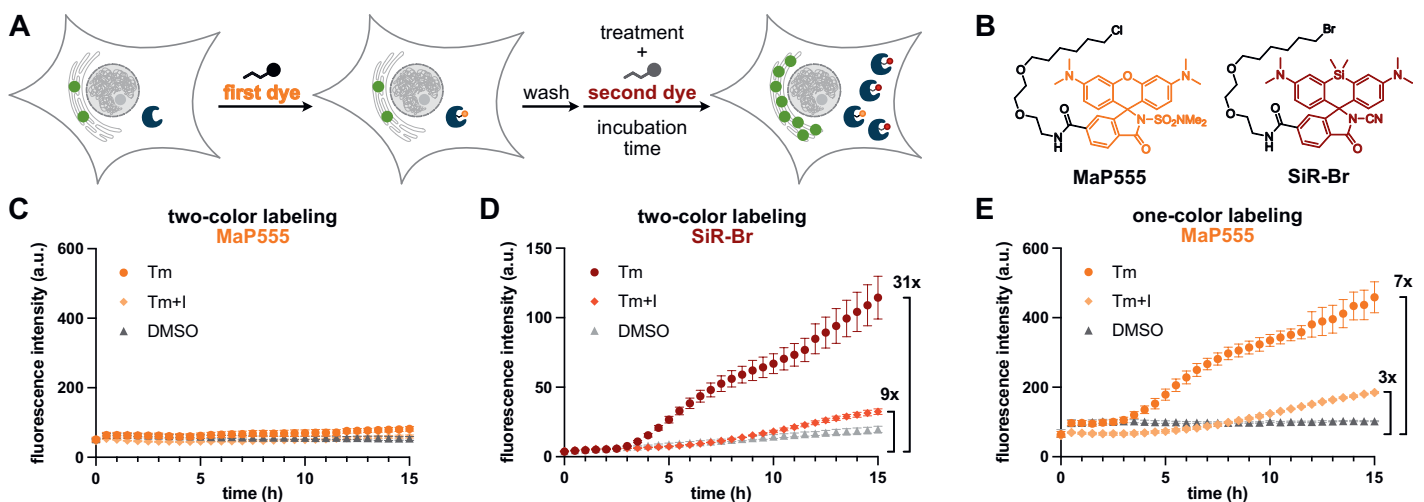


**Fig. 2.** Two-colour timestamping of BiP/GRP78 expression. **A** Schematic representation of sequential labelling steps. **B** Structures of MaP555 and SiR-Br. **C–E** HEK293-BiP-HT cells were incubated with MaP555 (100 nM, 30 min), washed, then incubated with three different treatments: DMSO (0.1%), Tm ( $2 \mu\text{g mL}^{-1}$ ), or Tm ( $2 \mu\text{g mL}^{-1}$ ) and PF-429242 (I, 10 mM), together with MaP555 (100 nM) or SiR-Br (100 nM). The fluorescence intensity in both channels (561 nm for MaP555 and 640 nm for SiR-Br) was measured over 15 h. For each condition and channel, intensity values from four different fields of view were plotted. Symbols represent the mean, error bars the standard deviation. Bars on the right indicate the dynamic range. **C** Two-colour labelling, MaP555 channel. **D** Two-colour labelling, SiR-Br channel. **E** One-color labelling, MaP555 channel. This figure was adapted from Ref. [10] with permission, Copyright 2025 Wiley-VCH GmbH.

probes absorb in yellow (MaP555) and red (SiR-Br) regions, enabling low-phototoxicity dual-channel imaging without bleed-through.

We applied this workflow to monitor BiP/GRP78 expression following Tm treatment (Fig. 2C–D). After Tm addition, MaP555 fluorescence remained constant, confirming efficient washing after the first labelling step. In contrast, the fluorescence intensity of SiR-Br, added together with Tm and remaining in the medium, increased significantly over time compared to DMSO-treated cells.

BiP/GRP78 expression is primarily induced through one of the UPR<sup>ER</sup> branches, the ATF6 pathway.<sup>[20]</sup> Using an inhibitor of this pathway, the site-1 protease inhibitor PF-429242,<sup>[21]</sup> together with Tm, resulted in a substantially reduced SiR-Br fluorescence increase compared to Tm alone, further confirming the regulation of HaloTag expression *via* BiP/GRP78.

The advantages of our two-color timestamping became apparent when comparing the dynamic ranges of one- and two-color imaging. One-color labelling using MaP555 in both labelling steps gave a dynamic range of 7 for Tm-treatment (Fig. 2E). With two-color labelling, however, we achieved a dynamic range of 31 (Fig. 2D). This improvement arises from the near-zero SiR-Br baseline after blocking of preexisting HaloTag with MaP555. The smaller increase in the presence of PF-429242 is more clearly distinguishable with two-color labelling (dynamic

range of 9 (two-color) compared to 3 (one-color)), showcasing the increased sensitivity of two-color labelling.

## 2.4 High-Content Screening for BiP/GRP78 Activators

BiP/GRP78 is an important chaperone in the ER, assisting the folding of proteins.<sup>[8]</sup> Therefore, its upregulation has been investigated in the context of diseases associated with the accumulation of misfolded proteins.<sup>[22]</sup> In a rat model of Parkinson's disease, the overexpression of BiP/GRP78 has been demonstrated to reduce  $\alpha$ -synuclein toxicity.<sup>[23]</sup> Thus, the discovery of small-molecule activators of BiP/GRP78 expression could be valuable in the search for treatments of proteinopathies.

To search for a novel activator of BiP/GRP78 expression, we carried out a high-content screening with a library of 7680 chemically diverse compounds at the biomolecular screening facility (BSF) at EPFL. The activity of the compounds was evaluated with a value calculated as a relative measure of activation based on controls (DMSO = 0, Tm = 1).

When we screened for high BiP/GRP78 expression, we found many compounds with a normalised value  $>0$  (Fig. 3A). Of these molecules, 320 (4% of 7680) compounds exhibited a score value of  $\geq 0.40$  and were thus selected as hits. In a repetition of the first round, 205 of these 320 hits were confirmed.

As BiP/GRP78 expression is activated *via* the UPR<sup>ER</sup>, compounds inducing general ER toxicity could lead to nonspecific activation. Therefore, we conducted a counter-screening in which we tested the compounds in the presence of the inhibitor PF-429242. Compounds whose activity depends on ATF6 pathway activation would show differential activation in this second screening round.

We performed the counter-screening with the 320 hits from the first screening round, normalising the fluorescence intensity between the controls Tm and Tm+PF-429242. Most compounds showed reduced activity in the presence of the inhibitor (Fig. 3B). We focused on the top 20 compounds that showed the largest difference between the two screening conditions, excluding 10 compounds that either had been previously reported as active structures or exhibited microscopy artifacts such as precipitation.

The remaining 10 hits represented structurally diverse molecules with no previously known BiP/GRP78-related activity (Fig. 3C). With RT-qPCR, we were able to validate one of these hits, the compound F2672–0399. Treatment with F2672–0399 resulted in a two-fold increase in BiP/GRP78 and HaloTag mRNA levels. This moderate level of upregulation is consistent with the design of the screen, which aimed to identify activators of BiP/GRP78 with reduced toxicity compared to strong ER stress inducers.

## 2.5 Advantages of Two-Color Timestamping

To evaluate the impact of the two-color strategy, we simulated conventional one-color labelling using only MaP555 for both labelling steps. At similar assay quality, the one-color approach would have missed 79% of the confirmed hits from the two-color screen, detecting only 43 of 205. Most importantly, F2672–0399, the RT-qPCR-validated hit, would have been overlooked.

For strong inducers like Tm, a one-color readout suffices. However, for the more subtle upregulation expected from low-toxicity hit compounds, the baseline subtraction achieved through timestamping is crucial.

## 3. Conclusions

We developed a chemigenetic gene expression reporter system based on the coexpression of the protein of interest BiP/GRP78 and the reporter HaloTag. By employing a two-color timestamping labelling, we achieved sensitive detection of changes in gene expression.

In addition to live-cell imaging, the system can be used in flow cytometry, allowing the correlation of basal and induced expression levels for a large number of cells.

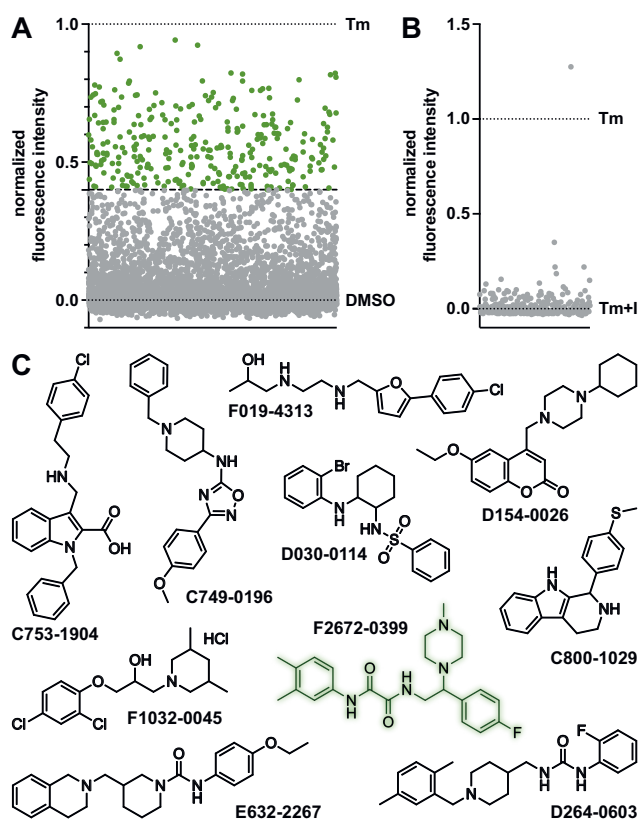


Fig. 3. High-content screening. **A** First round. HEK293-BiP-HT cells were incubated with MaP555 (100 nM, 30 min), washed, then incubated with 7680 screening compounds (10  $\mu$ M) and SiR-Br (100 nM) for 24 h. Plotted are the normalized values of all compounds,  $\geq 0.40$  in green,  $<0.40$  in grey (DMSO = 0, Tm = 1). **B** The 320 selected compounds were used in the second round, where the incubation procedure of the first round was repeated in the presence of PF-429242 (1, 10  $\mu$ M). Plotted are the average normalised values of all compounds (Tm + 1 = 0, Tm = 1). **C** Structures of 10 selected hits, F2672-0399 (validated by RT-qPCR) highlighted in green. This figure was adapted from Ref. [10] with permission, Copyright 2025 Wiley-VCH GmbH

While IRES-reporter assays exist,<sup>[12]</sup> our approach offers distinct advantages over previous BiP/GRP78 reporters, which typically employ promoter-driven luciferase or mGFP fusions.<sup>[24,25]</sup> These strategies either lack native genomic context or potentially compromise protein function. Our design preserves both BiP/GRP78 function and endogenous regulatory elements.

Compared to luciferase or fluorescent protein readouts, HaloTag enables modular dye selection for different applications. Although the two-color protocol requires additional labelling steps, batch pre-labelling before cell seeding mitigates this limitation. Finally, the system is adaptable to other genes, requiring only two modifications of the plasmids used for genome editing.

### Acknowledgements

H. L. thanks dsm-firmenich and the Swiss Chemical Society for the generous poster award. This work was supported by the Swiss National Science Foundation (PCEGP2\_186862). Genome sequencing was carried out at the Gene Expression Core Facility, and sequencing data analysis at the Bioinformatic Competence Center of EPFL. Primary screens performed at the Biomolecular Screening Facility of EPFL have been funded by the Swiss National Science Foundation through the NCCR Chemical Biology.

Received: January 29, 2026

- [1] T. I. Lee, R. A. Young, *Cell* **2013**, *152*, 1237, <https://doi.org/10.1016/j.cell.2013.02.014>.
- [2] G. S. Hotamisligil, R. J. Davis, *Cold Spring Harbor Perspect. Biol.* **2016**, *8*, a006072, <https://doi.org/10.1101/cshperspect.a006072>.
- [3] J. E. Bradner, D. Hnisz, R. A. Young, *Cell* **2017**, *168*, 629, <https://doi.org/10.1016/j.cell.2016.12.013>.
- [4] J. Cooper-Knock, J. Kirby, L. Ferraiuolo, P. R. Heath, M. Rattray, P. J. Shaw, *Nat. Rev. Neurol.* **2012**, *8*, 518, <https://doi.org/10.1038/nrneuro.2012.156>.
- [5] C. Hetz, *Nat. Rev. Mol. Cell Biol.* **2012**, *13*, 89, <https://doi.org/10.1038/nrm3270>.
- [6] D. Ron, P. Walter, *Nat. Rev. Mol. Cell Biol.* **2007**, *8*, 519, <https://doi.org/10.1038/nrm2199>.
- [7] C. Hetz, K. Zhang, R. J. Kaufman, *Nat. Rev. Mol. Cell Biol.* **2020**, *21*, 421, <https://doi.org/10.1038/s41580-020-0250-z>.
- [8] K. F. R. Pobre, G. J. Poet, L. M. Hendershot, *J. Biol. Chem.* **2019**, *294*, 2098, <https://doi.org/10.1074/jbc.REV118.002804>.
- [9] R. Damoiseaux, S. Hasson, Eds., 'Reporter gene assays', Humana New York, NY, New York, NY, **2018**, <https://doi.org/10.1007/978-1-4939-7724-6>.
- [10] H. Lämmermann, J. Nguyen, J. F. Tamez-Fernández, F. Kuttler, J. Bortoli Chapalay, M. Chambon, G. Turcatti, P. Rivera-Fuentes, *ChemBioChem* **2025**, *26*, e202500494, <https://doi.org/10.1002/cbic.202500494>.
- [11] S. K. Jang, H. G. Kräusslich, M. J. Nicklin, G. M. Duke, A. C. Palmenberg, E. Wimmer, *J. Virol.* **1988**, *62*, 2636, <https://doi.org/10.1128/jvi.62.8.2636-2643.1988>.
- [12] L. Lang, H.-F. Ding, X. Chen, S.-Y. Sun, G. Liu, C. Yan, *Chem. Biol.* **2015**, *22*, 957, <https://doi.org/10.1016/j.chembiol.2015.06.009>.
- [13] S. Nakade, T. Tsubota, Y. Sakane, S. Kume, N. Sakamoto, M. Obara, T. Daimon, H. Sezutsu, T. Yamamoto, T. Sakuma, K. T. Suzuki, *Nat. Commun.* **2014**, *5*, 5560, <https://doi.org/10.1038/ncomms6560>.
- [14] J. Pelletier, N. Sonenberg, *Nature* **1988**, *334*, 320, <https://doi.org/10.1038/334320a0>.
- [15] J. A. Vara, A. Portela, J. Ortin, A. Jiménez, *Nucleic Acids Res.* **1986**, *14*, 4617, <https://doi.org/10.1093/nar/14.11.4617>.
- [16] J. H. Kim, S.-R. Lee, L.-H. Li, H.-J. Park, J.-H. Park, K. Y. Lee, M.-K. Kim, B. A. Shin, S.-Y. Choi, *PLoS ONE* **2011**, *6*, e18556, <https://doi.org/10.1371/journal.pone.0018556>.
- [17] L. Wang, M. Tran, E. D'Este, J. Roberti, B. Koch, L. Xue, K. Johnsson, *Nat. Chem.* **2020**, *12*, 165, <https://doi.org/10.1038/s41557-019-0371-1>.
- [18] A. D. Elbein, *Annu. Rev. Biochem.* **1987**, *56*, 497, <https://doi.org/10.1146/annurev.bi.56.070187.002433>.
- [19] R. J. Kaufman, *Genes Dev.* **1999**, *13*, 1211, <https://doi.org/10.1101/gad.13.10.1211>.
- [20] M. D. Shoulders, L. M. Ryno, J. C. Genereux, J. J. Moresco, P. G. Tu, C. Wu, J. R. Yates, A. I. Su, J. W. Kelly, R. L. Wiseman, *Cell Rep.* **2013**, *3*, 1279, <https://doi.org/10.1016/j.celrep.2013.03.024>.
- [21] B. A. Hay, B. Abrams, A. Y. Zumbunn, J. J. Valentine, L. C. Warren, S. F. Petras, L. D. Shelly, A. Xia, A. H. Varghese, J. L. Hawkins, J. A. Van Camp, M. D. Robbins, K. Landschulz, H. J. Harwood, *Bioorg. Med. Chem. Lett.* **2007**, *17*, 4411, <https://doi.org/10.1016/j.bmcl.2007.06.031>.
- [22] V. Valenzuela, K. L. Jackson, S. P. Sardi, C. Hetz, *Mol. Ther.* **2018**, *26*, 1404, <https://doi.org/10.1016/j.ymthe.2018.04.004>.
- [23] M. S. Gorbatyuk, A. Shabashvili, W. Chen, C. Meyers, L. F. Sullivan, M. Salganik, J. H. Lin, A. S. Lewin, N. Muzyczka, O. S. Gorbatyuk, *Mol. Ther.* **2012**, *20*, 1327, <https://doi.org/10.1038/mt.2012.28>.
- [24] T. Kudo, S. Kanemoto, H. Hara, N. Morimoto, T. Morihara, R. Kimura, T. Tabira, K. Imaizumi, M. Takeda, *Cell Death Differ.* **2008**, *15*, 364, <https://doi.org/10.1038/sj.cdd.4402276>.
- [25] M. Kyeong, J. S. Lee, *Metab. Eng.* **2022**, *72*, 35, <https://doi.org/10.1016/j.ymben.2022.02.002>.

### License and Terms



This is an Open Access article under the terms of the Creative Commons Attribution License CC BY 4.0. The material may not be used for commercial purposes.

The license is subject to the CHIMIA terms and conditions: (<https://chimia.ch/chimia/about>).

The definitive version of this article is the electronic one that can be found at <https://doi.org/10.2533/chimia.2026.204>